Vietnam Journal of Catalysis and Adsorption
Tạp chí xúc tác và hấp phụ Việt Nam

https://chemeng.hust.edu.vn/jca/

Electrochemical synthesis of reduced graphene oxide and their anti-corosion properties

Hoang Van Hung*[1], Nguyen Thi Mo[1], and Pham Viet Phong[2]

[1] *Faculty of Chemistry, Hanoi National University of Education*
[2] *Le Loi Secondary School 432 Cat Bi, Hai An, Hai Phong*
**Email: hunghv@hnue.edu.vn*

ARTICLE INFO

Received: 12/5/2022
Accepted: 25/8/2022
Published: 28/8/2022

Keywords:
Reduced graphene oxide, corrosion protection, electrochemical synthesis.

ABSTRACT

Reduced graphene oxide (Gr) has been synthesized electrochemically on the surface of copper metal at a fixed potential of 1.5 V versus a standard saturated calomel electrode (SCE). The synthesized Gr was then characterized with X-Ray diffraction, thermogravimetric analysis, raman and Fourier transform infrared (FT-IR) spectroscopies. The anti-corrosion behavior of Gr was tested with polarization measurements and electrochemical impedance spectroscopy (EIS) in acidic medium of 0.5 M sulfuric acid solution. X-ray difraction (XRD), thermogravimetric analysis (TGA), and Raman analyses revealed that the Gr is more thermo-stable than GO. The *d*-spacing between sheets in comparison Gr (≈ *3.78 Å)* is shorter than *d*-spacing between sheets in GO (≈ *8.80 Å*). The Gr film synthesized within 30 seconds shows the better anti-corrosion behavior in comparison to the films synthesized with longer time interval.

Introduction

The refined metals have been used in many fields of human life in the form of alloys, but these forms of metals are often chemically reactive, requiring a coating to protect them from corrosion for many uses [1]. Corrosion protection of metals/alloys has developed to become an important branch which uses different approaches including coating with different kinds of organic films such as varnishes, paints, oxide and polymers; anodization; chemical modification and metal-coating or alloy coating [2]. However, almost of these methods have made a change in some physical properties of protected metals. The presence of the new materials makes a change in the dimensions of the metals because of the thickness of coating, the appearance and optical characteristics of metals, and generally reduces both thermal and electrical conductivity of metals. In order to overcome these problems, research to produce an ultrathin protective film with minimum change in physical properties of protected metals is demanded to develop [3].

The discovery of graphene with two-dimensional one-atom thick sheet of carbon has attracted so much attention in many different areas. The unique properties of graphene such as high chemical and thermal stability, chemical inertness, mechanical strength and impermeability have explored many technological and applications in industry [1]. The inertness and impermeability of graphene make it become a good barrier for corrosion protection of metals. In recent times, graphene films have been synthesized with CVD (chemical vapor deposition) method to act as an anticorrosion film [4]. However, this method is still complicated and costly. Searching a simpler method to produce graphene layer with a low cost is extremely exigent for industrial application.

https://doi.org/10.51316/jca.2023.011

In this work, we report a facile electrochemical method to synthesize graphene films on copper substrates. The anticorrosion behavior of graphene film was studied by potentiodynamic polarization and electrochemical impedance spectroscopy (EIS) measurements.

Experimental

Chemicals

The graphite (GR) flake was purchased from Sigma Aldrich. Aqueous solution or dispersion prepared using distilled water. All other chemicals used of analytical grade, obtained from China Chemical company and used without further purification.

Preparation of graphene oxide (GO)

Graphite flakes were oxidized chemically using a modified Hummer's method [5]. A mixture of 0.40 g graphite, 0.30 g KNO_3 and 10 mL of concentrated H_2SO_4 (98%) in a 100 mL beaker was stirred for 3.0 hours, following by slowly adding 0.50 g of solid $KMnO_4$. This mixture was then kept under vigorously stirring at 30°C for 7.0 hour and at 90°C for 4 hours. Finally, the whole mixture was added with 5.0 mL of 30% H_2O_2 solution; washed with 5% H_2SO_4 and bidistilled water for 6-8 times; filtered and dried at 80°C for 12 hours to obtain gray GO sheets.

Gr Coated Cu Electrode preparation

The Gr was synthesized on copper electrode as following: 200 mg of GO was dispersed in 200 mL of distilled water under 30 mins stirring and 30 mins ultrasonic conditions. The obtained dispersion was then used for electrochemical synthesis of Gr coated Cu electrode. In the electrochemical synthesis, a three-electrode cell connected to an Autolab PGS-302N potentiostat/galvanostat instrument supplied by Metrohm AUTOLAB, Netherland was employed, in which Cu disk electrode with diameter of 2 mm employed as working electrode, saturated calomel electrode served as reference electrode and sheet platinum electrode employed as auxiliary/counter electrode. The Gr was synthesized potentiostatically at a fixed potential of 1.50 V versus standard SCE and with different time intervals. In order to collect Gr for different characterizations, larger sheet electrode (1cm × 3cm) of copper was used and the electrolyzing time was kept longer. The Gr coated electrodes were then rinsed gently and dried under ambient condition.

Characterization

All studied samples ware characterized with an Brucker D5005 X-ray diffractometer with the wavelength of Kα-radiation of 1.5406 Å. The DTG-60H instrument (Shimazu, Japan) was used to study thermal stability of synthesized materials. The thermogravimetric analysis (TGA) data were acquired under air flow of 50 mL second^{-1} and at a heating rate of 10°/min. Fourier transform infrared spectroscopy (FT-IR) was performed on NEXUS-670, Nicotet – USA. Raman spectra were recorded from LAB RAM HR800, HORIBA-France.

Electrochemical method

Cathodic and anodic polarization curves were potentiodynamically recorded with the scan rate of 5 mV s^{-1} using a conventional three-electrode cell connected to an Autolab PGS-302N potentiostat/galvanostat instrument supplied by Metrohm AUTOLAB, Netherland. The disc electrode of copper with a diameter of 2.0 mm was served as a working electrode (WE), a platinum rod was used as counter/auxiliary electrode and a standard saturated calomel electrode (SCE) was served as the reference electrode. All experiments were performed at ambient condition. The working electrode (WE) was polished mechanically with different emery papers up to 1000 grade. After polishing, the electrode was rinsed several times with double distilled water, degreased with ethanol and dried. The measurements related to electrochemical impedance spectroscopy (EIS) were performed using an electrochemical system and instruments similar to that used in polarization measurements with perturbation amplitude of 10 mV and frequency range between 1 Hz to 100 kHz. Electrochemical impedance data were fitted using assumed equivalent circuit with NOVA software version 2.0.

Results and discussion

Characterization

Thermogravimetric analysis

The thermal stability of materials can be investigated easily with thermogravimetric analysis (TGA). Figure 1 shows TGA curve of GO and Gr. As can be seen, all the materials show a small mass loss at the temperature below 190°C (about 18% for GO and 20% for Gr) due to the de-intercalation of H_2O from GO and Gr [6]. GO with

https://doi.org/10.51316/jca.2023.011

functionalities on the graphene sheets; most of the mass (85.0%) was lost at the relatively low temperature of about 191°C. This could be explained because of the ease of pyrolysis of labile oxygen-containing groups leading to the strong release of water vapor, CO_2 and CO gases, and thus causing the large mass loss [7, 8]. In contrast to GO, TGA diagram of graphene shows the significant improvement in thermal stability, which proves that the oxygen-containing groups in GO sheets were removed in the reduction step [9, 10]. The thermal stability of Gr depends on the number of residue functional groups. The fewer functional groups the Gr has, the more stable the Gr is. Gr with fewer functional groups, the d-spacing between graphene sheets will be shortened therefore Gr will be more stable. From the TGA curves, it is interesting that there are two peaks appearing at 215°C and 407°C corresponding to two main mass lost processes happening at these temperatures. This may be explained that oxygen functional groups on carbon sheets of GO were continuously reduced at surface of electrode during electrochemical processes at anode, therefore the earlier sheets were reduced much more than the later sheets. It means that the later sheets will have more functional groups, therefore are less stable and are decomposed at lower temperature of about 215°C. However, this temperature is still slightly higher than the decomposition temperature of GO sheets (191°C), which were not yet reduced.

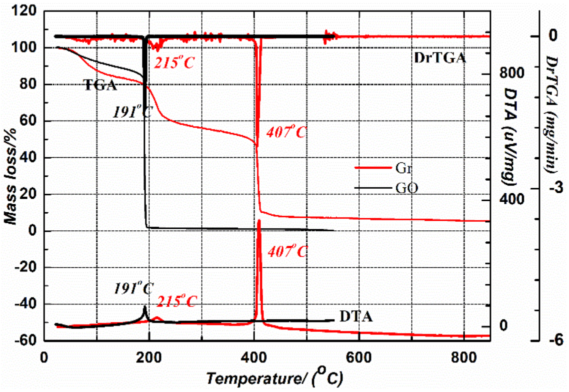

Figure 1: TGA diagram of GO and Gr

X-ray diffraction (XRD)

Figure 2 represents the XRD patterns of studied samples including graphite, GO and Gr. The *d*-spacings of graphite, graphene oxide and Gr were calculated from values of 2θ angular of the observed reflection peaks using the Bragg equation $\lambda = 2d \sin\theta$, where λ is X-ray radiation wavelength and θ is scattering angle [10, 11]. As can be seen, a dominate sharp peak appears at 2θ = 26.5° correlating to d-spacing of 3.36 Å in the XRD pattern of graphite. Meanwhile, two peaks appear at lower angle in the XRD pattern of GO (one at 2θ = 11° and other at 2θ = 22.5° correlated to *d*-spacing between layers of 8.80 and 3.95 Å, respectively) showing an increase of *d*-spacing between carbon sheets of GO. This increase can be explained due to the formation of functional groups on carbon sheets during oxidizing processes of pristine graphite. In the case of Gr, there is a broad peak appearing at 2θ = 23.5° corresponding to an interlayer space *d* = 3.78 Å, which is in lying in between the d-spacing of graphite and grapheme oxide. This value of d-spacing suggests that there is still existence of residue oxygen functional groups in carbon sheets leading to slightly higher value of d-spacing in comparison to the case of graphite [12].

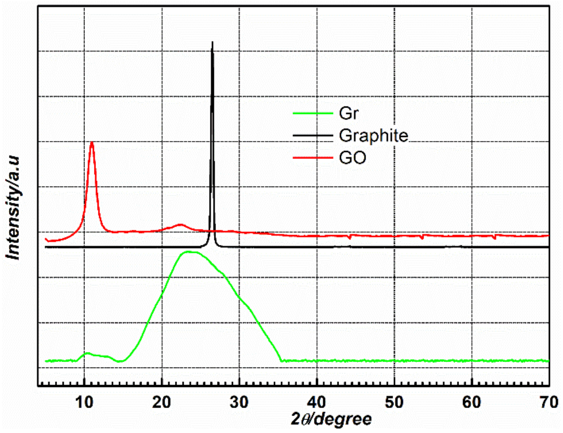

Figure 2: X-ray diffraction patterns of pristine graphite GO and Gr

Raman spectroscopy

Raman spectrum can give information used evaluate further characteristics of GO and Gr because, in general, there are two dominate sharp peaks at 1344 and 1600 cm^{-1} called D and G bands, respectively. The D band is assigned to the breathing mode of κ-point phonons of A_{1g} symmetry, while G band is corresponding to E_{2g} phonon of sp^2 bonds of carbon atoms [13]. The intensity of these peaks depends on the structure of the carbon sheets. As shown in the Fig 3, both spectra of GO and Gr consist of D and G bands. However, the intensity ratio between D and G peaks of GO (I_D/I_G = 0.87) is smaller than that of Gr (I_D/I_G = 1.41), which indicates an increase of sp^2 domain number after reduction of GO to form Gr, a decrease in edge planes and the degree of odorless in the Gr sheets, which relates to a decrease of number of functional groups during the electrochemical processes at anode of GO to Gr [13, 14]. This result is well agreed with results reported in literatures [15, 16] and one more time proves that Gr was formed electrochemically on Cu surface.

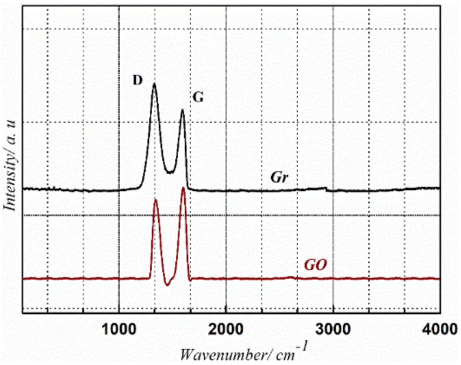

Figure 3: Raman Spectra of *GO and Gr*

Fourier Transform Infrared (FT-IR) Spectroscopy

FT-IR spectrum of a material is one which can be used effectively to analyse the characteristics of the material. Figure 4 shows FT-IR spectra of GO and Gr. As can be seen, two spectra of GO and Gr are similar. Both spectra represent a broad absorption band between 3000 and 3500 cm^{-1}, assigned to hydroxyl group of adsorbed water molecules. Similarly, two absorption bands at 1616 and 1716 cm^{-1} corresponding to the vibration of C=C bond present in carbon ring of graphene sheet and the vibration of C=O bond in carboxyl group on surface of carbon sheet. At smaller value of wavenumber, the absorption bands at 1060 and 1242 cm^{-1} are assigned to the vibration of C – O – C groups on surface of graphene sheets and C – O stretching vibration, respectively [17]. The obtained result is in good agreement with result obtained from Raman spectra, proves that there are still functional groups on graphene sheets [18].

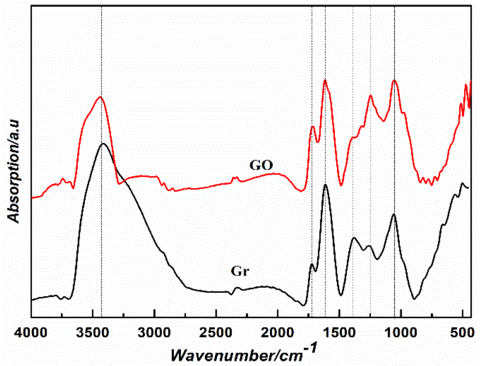

Figure 4: FT-IR spectra of Gr and GO materials

Corrosion test

Polarization measurements

The Gr coated copper electrodes were then naturally dried in the air and used as working electrodes in the polarization and electrochemical impedance measurements. Figure 5 displays polarization measurements in term of Tafel plot, in 0.5M sulfuric acid medium of Gr coated copper electrodes synthesized at the constant voltage of 1.5V. The measured samples are denoted as CuGrX (where X is the synthesis time of Gr measured in minute) and the uncoated Cu sample is designated as "bare Cu".

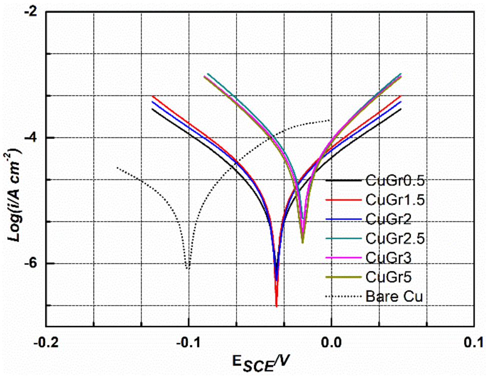

Figure 5: Tafel plot of CuGrX electrodes synthesized at 1.5V

Table 1: *Values of corrosion current density (i_{corr}/A cm^{-2}), corrosion potential (E_{corr}/mV versus E_{SCE}) Tafel (β_a and β_b/V decade^{-1}), corrosion rate (C_R/ mm year^{-1}), polarization resistance (R_P/Ω) of Gr coated Cu electrodes calculated from Tafel curves*

Sample	*i*/10^{-6}	β_a	-β_c	*r*/10^{-2}	*Rp*	E_{corr}
Bare Cu	3.45	0.038	0.024	4.05	1823	-100
CuGr0.5	1.04	0.008	0.013	1.2	2154	-40
CuGr1.5	2.48	0.014	0.016	2.9	1334	-40
CuGr2	2.98	0.016	0.019	3.5	1304	-40
CuGr2.5	11.6	0.026	0.020	13.5	422	-20
CuGr3	10.8	0.027	0.020	12.6	465	-20
CuGr5	7.31	0.019	0.014	8.5	480	-20

The corrosion potential (E_{corr}), Tafel slopes (β_a and β_b) and corrosion current (I_{CORR}) were determined from polarization curves in term of Tafel curves. The corrosion rate (C_R measured in millimeters per year, MPY) was determined from I_{CORR} using equation [15, 19-21, 22]:

$$C_R = K \times \frac{(EM) \times i_{CORR}}{F \times d}$$

where *K* is conversion constant (convert cm/s to mm/year, $K = 3.15\times10^8$), *EM* is the equivalent mass (g/equiv), *F* is Faraday constant (96500 Coulomb/equiv) and *d* is density of Cu (8.90 g/cm^3). The calculated values corresponding to the Figure 5 listed in Table 1 show that the coating of Gr on Cu metal changes the corrosion rate of Cu metal in 0.5M sulfuric acid solution. All Gr coated Cu show the anodic protection with the anodic shifting potential from 60 to 80 mV, in which CuGr2.5, CuGr3 and CuGr5 samples have an anodic shift of 80 mV, higher than the shift of the rest samples. When the Gr coating time was up to 0.5 minutes (30 seconds), the Cu corrosion rate was significantly reduced from 4.05 × 10^{-2} mm $year^{-1}$ to 1.20 × 10^{-2} mm $year^{-1}$ (about 3.4 times). Thus, it can be said that Gr coating can prevent corrosion of Cu in 0.5M sulfuric acid environment. However, if coating time is continuing to increase to 1.5 and 2.0 minutes, the corrosion rate is increased compared to the 0.5 minutes case though the corrosion rate is still reduced compared to the bare Cu electrode. The reason for this abnormality can be explained due to the oxidation of Cu surface at anode occurring simultaneously with the reduction of graphene oxide producing the smoothless surface of Cu. This leads to the aggregation of electrolyte at the surface of Cu metals and the facilitation of the corrosion process.

Electrochemical Impedance Spectroscopy (EIS)

EIS is a powerful technique which has been used effectively to studied corrosion protection of metals [19]. Nyquist form for the bare Cu electrode and Gr coated with different synthesis time intervals recorded at OCP in 0.50 M sulfuric acid solution are depicted in Fig.7. The charge-transfer resistance R_{CT} and double layer capacitance C_{DL} values determined by fitting of impedance measurement data using 2.0 NOVA software and equivalence circuit as shown in Figure 6, are given in Table 2.

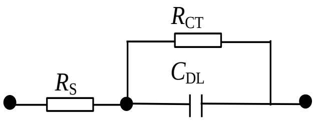

Figure 6: Equivalence circuit used for fitting experimental data

The values of R_{CT} obtained from electrochemical impredance measurements shown in Tab 2. are in good agreemnet with values obtained from polarization measurements. The R_{CT} reaches maximum value of 593 Ω when Gr coating time is of 30 seconds and double layer capacitance get the minimum value of 0.2 *µC*.

As explained in previous part, there is an oxidation of Cu during the formation of Gr and this oxidation of Cu increases as coating time increases leading to a decrease of R_{TC} value. Though the magnitude of resistances obtained from polarization measurement is higher than resistances obtained from impedance measurements, these values have the same trend. This difference may be explained that in the polarization measurement, the polarization resistance is a sum of resistances of all ohmic elements present in the electrochemical system, including solution, metal surface and double layer of interface between electrolyte and surface of electrode. While, charge transfer resistance obtained in the electrochemical impedance measurement.

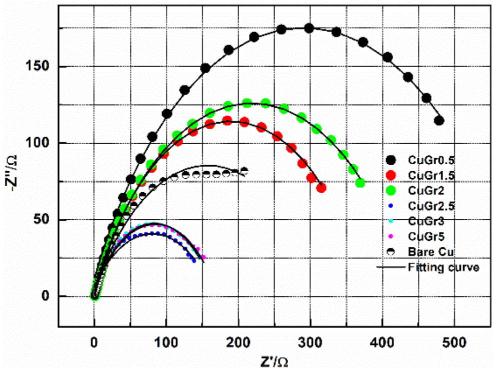

Figure 7: Nyquist diagrams of bare Cu and CuGrX samples

Table 2: values of charge transfer resistance (R_{CT}/Ω) and double layer capacitance (C_{DL}/mF) calculated from EIS data of Gr electrodes

Sample	*C_{DL}/µC*	*R_{CT}/Ω*
Bare Cu	0.6	364
CuGr0.5	0.2	593
CuGr1.5	0.6	371
CuGr2	0.4	444
CuGr2.5	0.7	168
CuGr3	0.7	169

The porosity of the Gr layer can be easily observed by the valued of double layer capacitance. As presented on the Table 2, the electrode coated with 30 seconds gives the minimum value of capacitance (µC), while this value increases for the electrode with longer coating time. The increase in double layer capacitance reduces charge transfer resistance, and therefore reduces the corrosion protection yield [23].

Conclusion

We have represented the electrochemical mothod to synthesize reduced graphene, its characterisitics as well as anti-corrosion on copper surface. The obtained characteristics of Gr showed that the electrochemically synthesized Gr is more thermal stable than graphene oxide. The Gr, with *d*-spacing between sheets of 3.78 *Å*, is completetely burned at 407°C, while graphene oxide with *d*-spacing between sheets of 8.80 *Å*, is burned completely at 191ºC. The reduction of oxygen functional group on the sheets of GO shortens the *d*-spacing between sheets in the Gr. This result can also be observed in the raman spectra of GO (I_D/I_G = 1.41) and Gr (I_D/I_G = 0.8). The Gr film coated with 30 seconds shows the significant anti-corrosion behavior which can be seen in both electrochemical inpedance and polarization measurements.

References

1. M. A. Al-Sammarraie and M. H. Raheema, International Journal of Corrosion, 2017 https://doi.org/10.1155/2017/6939354
2. N. U. Kiran, S. Dey, B. P. Singh and L. Besra, Coatings 7 12 (2017) 214.
3. J. Chen, C. Li, W. Cao, S. Sang, Q. Wu, H. Liu and K. Liu, Ionics 25 (2019) 2935–2944.
4. D. Prasai, J. C. Tuberquia, R. R. Harl, G. K Jennings and K. I. Bolotin, ACS Nano 6 2 (2012) 102-1108.
5. G. Williams, B. Seger, P. V. Kamat, ACS Nano 2 (2008) 1487–1491.
6. K. Zhang, L. L. Zhang, X. S. Zhao, J. Wu, J. Chem. Mater. 22 4 (2010) 1392-14301.
7. S. Stankovich, D. A. Dikin, R. D. Piner, K. A. Kojhaas, A. Kleinhammes, Y. Jia, Y. Wu, S. B. Nguyen, R. S. Ruoff, Carbon 45 (2007) 1558-1565.
8. M. Shi, J. Shen, H. Ma, Z. Li, Z. Lu, N. Li, M. Ye, Colloids and Surface A: Physicochem. Eng. Aspects 405 (2012) 30-37.
9. Z. Huimin, S. Fang, F. Xinfei, Y. Hongtao, W. Dan, Q. Xie, Chin. J. Catal. 33 (2012) 777-782.
10. H. V. Hoang, R. Holze, Chem. Mater. 18 (2006) 1976-1980.
11. T. X. Nguyen, M. T. Nguyen, H. V. Nguyen, H. V. Hoang, Asian. J. Chem. 28 6 (2016) 1297-1303.
12. A. V. vel M. Rugan, T. M. Raliganth, and A. Manthiram, Rapid, Chem. Mater. 21 (2009) 5004 – 5006.
13. Y. Min, K. Zhang, W. Zhao, F. Zheng, Y. Chen, Y Zhan, Chemical Engineering Journal 203 (2012) 183-194.
14. Q. Wei, T. Fu, Q. Yue, H. Liu, S. Ma, M. Cai, F. Zhou, Tribology International 157 (2021) 106895 1-10.
15. S. C. Sahu, A. K. Samantara, M. Seth, S. Parwaiz, B. P. Singh, P. C. Rath, B. K. Jen, Electrochemistry Communications 32 (2013) 22-26.
16. S. Pei, H.-M. Cheng, Carbon 50 (2012) 3210-3228.
17. X. Liu, L. Pan, Q. Zhao, T. Lv, G. Zhu, T. Chen, Ting Lu, Z. Sun, C. Sun, Chem. Eng. J. 183 (2012) 283-243.
18. B. P. Singh, S. Nayak, K. K. Nanda, B. K. Jena, A. Bhattacharjee, L. Besra, Carbon 61 (2013) 47-56.
19. S. Shreepathi, H. V. Hung, R. Holze, Journal of The Electrochemical Society 154 2 (2007) C67-C73.
20. D. Prasai, J. C. Tuberquia, R. R. Harl, D. K. Jennings, ACS Nano 6 2 (2012) 1102-1108.
21. Peres. N., Electrochemistry and Corrosion Science, Kluwer Academic Publishers, NewYork 2004 92.
22. H. Tan, D. Wang, Y. Guo, Anti-Corrosion Methods and Materials 66 6 (2019) 853 – 860.
23. L. R. Chauhan, G. Gunasekaran, Corrosion Science 49 (2007) 1143-1161.